Available online at www.sciencedirect.com

ScienceDirect

Procedia Computer Science 108C (2017) 1453–1462

Procedia Computer Science

International Conference on Computational Science, ICCS 2017, 12-14 June 2017, Zurich, Switzerland

Pareto Ranking Bisection Algorithm for EM-Driven Multi-Objective Design of Antennas in Highly-Dimensional Parameter Spaces

Adrian Bekasiewicz[1,2*†], Slawomir Koziel[1,2‡§], Leifur Leifsson[3**], and Xiaosong Du[3††]

[1]*Reykjavik University, Reykjavik, Iceland.*
[2]*Gdansk University of Technology, Gdansk, Poland.*
[3]*Iowa State University, Ames, Iowa, USA.*
bekasiewicz@ru.is, koziel@ru.is, leifur@iastate.edu, xiaosong@iastate.edu

Abstract

A deterministic technique for fast surrogate-assisted multi-objective design optimization of antennas in highly-dimensional parameters spaces has been discussed. In this two-stage approach, the initial approximation of the Pareto set representing the best compromise between conflicting objectives is obtained using a bisection algorithm which finds new Pareto-optimal designs by dividing the line segments interconnecting previously found optimal points, and executing poll-type search that involves Pareto ranking. The initial Pareto front is generated at the level of the coarsely-discretized EM model of the antenna. In the second stage of the algorithm, the high-fidelity Pareto designs are obtained through optimization of corrected local-approximation models. The considered optimization method is verified using a 17-variable uniplanar antenna operating in ultra-wideband frequency range. The method is compared to three state-of-the-art surrogate-assisted multi-objective optimization algorithms.

Peer-review under responsibility of the scientific committee of the International Conference on Computational Science

Keywords: antenna design, multi-objective optimization, EM-driven design, bisection algorithm, variable-fidelity simulations, surrogate modeling

* Engineering Optimization and Modeling Center, School of Science and Engineering
† Faculty of Electronics Telecommunications and Informatics
‡ Engineering Optimization and Modeling Center, School of Science and Engineering
§ Faculty of Electronics Telecommunications and Informatics
** Department of Aerospace Engineering
†† Department of Aerospace Engineering

1877-0509
Peer-review under responsibility of the scientific committee of the International Conference on Computational Science
10.1016/j.procs.2017.05.102

1 Introduction

Complex geometry of modern antenna structures is a result of strict requirements imposed on their electrical and/or field performance figures, as well as small size of modern communication systems. Size reduction of ultra-wideband (UWB) antennas is often achieved as a result of various topological modifications such as ground plane slots and stubs that enlarge the current path within the structure (Li, Cheung et al. 2013), as well as feed line alterations that increase the impedance bandwidth (Bekasiewicz and Koziel, 2015). Band-notch functionality, on the other hand, is often realized using slots within the radiator or various resonators allocated in the vicinity (Li et al. 2012) or below the feed line (Nouri and DadashZadeh, 2011).

Complex antenna structures are characterized by a large number of design parameters (Bekasiewicz and Koziel, 2015). Also, they can be accurately evaluated only by means of numerically expensive high-fidelity electromagnetic (EM) solvers. For the sake of design reliability, environmental components such as connectors (Khan et al. 2016), housing (Alsath and Kanagasabai, 2015), or fixtures (Liu et al. 2012) are often included into EM models, which additionally increases their evaluation cost. These factors make EM-driven design of modern antennas a challenging task. Typically, it is handled manually by means of visual inspection of the structure response intertwined with sweeping of its parameters (usually one at a time). Although very laborious and unable to identify truly optimum designs, manual design is still considered as a reasonable compromise between computational feasibility and efficiency. On the other hand, conventional optimization driven by local (e.g., gradient-based, or derivative free, see: Nocedal and Wright, 2006; Conn et al. 2009) or global (e.g., genetic algorithms, or simulated annealing, see Ding et al. 2008; Martinez-Fernandez et al. 2007) methods are numerically prohibitive due to a large number of EM model evaluations required to complete the process.

Antenna design normally involves several performance figures (e.g., maximization of in-band gain (Kuwahara, 2005), minimization of reflection (Bekasiewicz and Koziel, 2015), front-to-back ratio (Koziel and Bekasiewicz, 2015), or antenna size (Koziel and Ogurtsov, 2013)) that have to be simultaneously taken into account. These requirements often stay in conflict with each other meaning that improvement of one of them is not possible without degradation of the others. For the sake of simplicity, design requirements are often aggregated into a single-objective task using appropriate weighting factors which allows for solving the problem using conventional optimization algorithms. However, comprehensive information about trade-offs between various objectives (referred to as a Pareto front) may be only obtained by means of genuine multi-objective optimization (Deb, 2001). The most popular methods for solving multi-objective design problems are population-based metaheuristics (e.g., evolutionary, or firefly algorithms, see e.g., Koziel and Ogurtsov, 2013; Yang, 2013). Although metaheuristics allow for generating the entire Pareto set in a single algorithm run, they typically require thousands of model evaluations to complete the optimization process (Kuwahara, 2005). Thus, they are unsuitable for handling expensive high-fidelity EM simulation models of antenna structures.

The cost of antenna design can be reduced using surrogate-assisted techniques, where the optimization is executed at the level of a coarsely-discretized EM model of the structure at hand. The optimized design is further corrected using occasionally acquired accurate EM model data. A variety of surrogate-based methods have been successfully utilized for rapid antenna design. These include, among others, space mapping (Koziel and Ogurtsov, 2013), manifold mapping (Koziel et al. 2013), shape preserving response prediction (Koziel et al. 2012), adaptive response correction (Koziel and Ogurtsov, 2014), and, recently, utilization of response features (Koziel and Bandler, 2015). The mentioned approaches allow for obtaining optimal design solutions at a cost corresponding to a few dozens of high-fidelity EM model simulations.

Several surrogate-assisted methods for fast EM-driven multi-objective design of antenna structures have been proposed. In (Koziel and Ogurtsov, 2013), the Pareto set has been obtained by metaheuristic optimization of an auxiliary response surface approximation model constructed from the low-fidelity EM model data. The high-fidelity representation of the Pareto front has been subsequently obtained

through space mapping correction of the selected designs. An alternative refinement strategy based on co-kriging has been proposed in (Koziel et al. 2014a). Moreover, design space reduction schemes have been proposed in (Koziel et al. 2014b; Koziel and Bekasiewicz, 2016a) to extend applicability of the approach to highly-dimensional problems. These techniques, however, exploit a stochastic algorithm at certain stage of the design process. A fully deterministic method for generating Pareto set, a so-called sequential domain patching algorithm has been proposed in (Koziel and Bekasiewicz, 2016a). Another approach that identifies the Pareto front representation in a point-by-point manner has been reported in (Koziel and Bekasiewicz, 2016c).

Recently, a Pareto ranking bisection algorithm (PRBA) for multi-objective optimization of modern antennas has been introduced in (Koziel and Bekasiewicz, 2017). PRBA is a two stage method that generates initial approximations of the Pareto designs using bisection algorithm. The candidate solutions are then locally improved by means of a grid-restricted search involving Pareto ranking. Low cost of the design process is ensured by performing the search at the coarsely-discretized EM model level. The high-fidelity EM representation of the Pareto front is found, similarly as in (Koziel and Bekasiewicz, 2016a), i.e., by optimization of local approximation surrogates generated around the designs found by PRBA.

In this work, a numerical study concerning feasibility of PRBA for multi-objective optimization of a numerically expensive antenna models in highly-dimensional spaces is performed. The benchmark problem is a 17-variable uniplanar UWB structure optimized with respect to two conflicting design requirements, i.e., minimization of in-band reflection and size reduction. The method is extensively compared against state-of-the-art surrogate-assisted multi-objective optimization algorithms. This is the first attempt to investigate robustness of the PRBA approach for a design problem with over a dozen design variables.

2 Multi-Objective Optimization Using PRBA

In this section, we recall the details of the considered Pareto ranking bisection algorithm. Specifically, we discuss the multi-objective optimization problem formulation, as well as describe the PRBA approach. The section is concluded with a brief explanation of the utilized response correction approach. A design example and comparison of PRBA to benchmark algorithms is provided in Section 3.

2.1 Multi-Objective Problem Formulation

Let $\boldsymbol{x}$ denote a vector of the antenna design parameters and $\boldsymbol{R}_f(\boldsymbol{x})$ represent a response of its high-fidelity EM simulation model. Then, let $F_k(\boldsymbol{R}_f(\boldsymbol{x}))$, $k = 1, \ldots, N_{obj}$, be a kth design objective. Design objectives can be defined with respect to antenna in-band reflection, gain, phase stability, size, etc. If $N_{obj} > 1$, comparison of the solutions is realized using a dominance relation (Deb, 2001). We say that $\boldsymbol{y} \prec \boldsymbol{x}$ ($\boldsymbol{y}$ dominates over $\boldsymbol{x}$) if $F_k(\boldsymbol{R}_f(\boldsymbol{y})) \leq F_k(\boldsymbol{R}_f(\boldsymbol{x}))$ for all $k = 1, \ldots, N_{obj}$, and $F_k(\boldsymbol{R}_f(\boldsymbol{y})) < F_k(\boldsymbol{R}_f(\boldsymbol{x}))$ for at least one k. The goal of the multi-objective optimization is to find a Pareto set X_P composed of non-dominated designs so that for any $\boldsymbol{x} \in X_P$ there is no $\boldsymbol{y}$ for which $\boldsymbol{y} \prec \boldsymbol{x}$ (Deb, 2001). The set X_P represents the best possible compromise between the considered objectives.

For the purpose of subsequent considerations, we also define a Pareto ranking concept. Let $X = \{\boldsymbol{x}_1, \ldots, \boldsymbol{x}_n\}$ be a set of designs. Pareto ranking of the design $\boldsymbol{x}_k \in X$ with respect to X is the number of designs from X that dominate over $\boldsymbol{x}_k$.

2.2 Pareto Ranking Bisection Algorithm

The Pareto front normally resides in the very small region of the search space, allocation of which is unknown beforehand. Therefore, the first step of the considered multi-objective optimization procedure is identification of the extreme Pareto-optimal designs (Koziel et al. 2014b). These are obtained through sequential single-objective optimizations with respect to one design requirement at a time. Low computational cost of the process is ensured by identification of the extreme points at the coarsely-discretized EM model level of the antenna by solving

$$\boldsymbol{x}_k^* = \arg\min_{\boldsymbol{x}} F_k\left(\boldsymbol{R}_c(\boldsymbol{x})\right) \tag{1}$$

for $k = 1, \ldots, N_{obj}$ (Koziel et al. 2014b). Depending on the number of antenna design parameters, the cost of solving (1) varies from a few dozens to over a hundred evaluations of the low-fidelity model $\boldsymbol{R}_c$ per objective.

Initial approximation of the Pareto front is obtained using the PRBA method (Koziel and Bekasiewicz, 2017). The algorithm is formulted for bi-objective problems. The following notation is used (n is the design space dimensionality):

- $\boldsymbol{x}_{c.0.1} = \boldsymbol{x}_1^*$ and $\boldsymbol{x}_{c.0.2} = \boldsymbol{x}_2^*$ – extreme Pareto designs;
- $\boldsymbol{x}_{c.i.k}$ – kth (approximate) Pareto design found in the ith algorithm iteration; the number of new designs found in iteration i is $K_i = 2^{i-1}$; the total number of designs after ith iteration is $N_i = 2^i+1$;
- $\boldsymbol{d} = [d_1 \ldots d_n]^T$ – perturbation size (user defined parameter);
- M – maximum number of PRBA iterations;
- $\boldsymbol{m} = [m_1 \ldots m_M]^T$ – number of bisections in subsequent iterations.

The algorithm flow is as follows:

1. Set $i = 1$;
2. Find initial approximations of the candidate Pareto designs by performing bisections $\boldsymbol{x}_{c.i.k} = [\boldsymbol{x}_{c.i-1.k} + \boldsymbol{x}_{c.i-1.k+1}]/2$, $k = 1, \ldots, K_i$;
3. Set $m = 1$;
4. For each $k = 1, \ldots, K_i$, evaluate $2n$ perturbations of the size $\boldsymbol{d}$ around $\boldsymbol{x}_{c.i.k}$; for each design, calculate its Pareto ranking and select the one with the lowest value as a new $\boldsymbol{x}_{c.i.k}$;
5. Set $m = m + 1$; if $m \le m_i$ go to 4;
6. Concatenate sets $\{\boldsymbol{x}_{c.i-1.k}\}_{k = 1, \ldots, Ki-1}$ and $\{\boldsymbol{x}_{c.i.k}\}_{k = 1, \ldots, Ki}$ as follows $\{\boldsymbol{x}_{c.i-1.1}\ \boldsymbol{x}_{c.i.1}\ \boldsymbol{x}_{c.i-1.2}\ \boldsymbol{x}_{c.i.2}\ \boldsymbol{x}_{c.i-1.3}\ \ldots\ \boldsymbol{x}_{c.i-1.Ki-1}\ \boldsymbol{x}_{c.i.Ki}\}$ and re-index designs accordingly;
7. Set $i = i + 1$; if $i \le M$ go to 2; otherwise return the Pareto set (denoted as $\boldsymbol{x}_c^{(k)}$, $k = 1, \ldots, N_M$);

Conceptual illustration of PRBA is shown in Fig. 1. The algorithm generates the initial (low-fidelity) Pareto set composed of $N_M = 2^M + 1$ designs. Note that the poll-search involving Pareto ranking allows for local improvements (in multi-objective sense) of the candidate designs obtained through bisections. The initial Pareto front representation is further refined to the high-fidelity model level using local approximation models (cf. Section 2.3).

As mentioned before, the perturbation size vector $\boldsymbol{d}$ is a user-defined parameter. Here, it is given as $\boldsymbol{d} = |\boldsymbol{x}_1^* - \boldsymbol{x}_2^*|/N_M$, with N_M being the number of Pareto-optimal designs. Such a formulation ensures that the perturbation size in each dimension is constant and corresponds to the distance between the two neighboring Pareto designs found by PRBA.

The numerical cost of PRBA is $M_\Sigma(2n + 1) - M$, where $M_\Sigma = \sum_{k = 1,\ldots,M} m_k$. Thus, for $n = 15$, $M = 3$ (which corresponds to a 9-element Pareto set), and $\boldsymbol{m} = [3\ 2\ 1]$, PRBA requires 183 model evaluations to find the low-fidelity Pareto front representation. Note that m_k gradually decreases because the expected relocations of designs due to Step 4 of the algorithm are getting smaller. The reason is that $\|\boldsymbol{x}_{c.i-1.k} - \boldsymbol{x}_{c.i-1.k+1}\|$ is approximately twice smaller in each iteration.

2.3 Pareto-Set Refinement Using Local Surrogates

The algorithm of Section 2.2 identifies Pareto set and the low-fidelity model level $\boldsymbol{R}_c$. The high-fidelity Pareto set is identified by refining the designs $\boldsymbol{x}_c^{(k)}$, $k = 1, \ldots, N_M$, using the output space mapping (OSM) algorithm (Koziel and Ogurtsov, 2013). The refinement procedure is formulated as

$$\boldsymbol{x}_f^{(k)} \leftarrow \arg \min_{\boldsymbol{x},\, F_2(\boldsymbol{x}) \le F_2(\boldsymbol{x}_f^{(k)})} F_1\left(\boldsymbol{R}_s(\boldsymbol{x}) + [\boldsymbol{R}_f(\boldsymbol{x}_f^{(k)}) - \boldsymbol{R}_s(\boldsymbol{x}_f^{(k)})]\right) \tag{2}$$

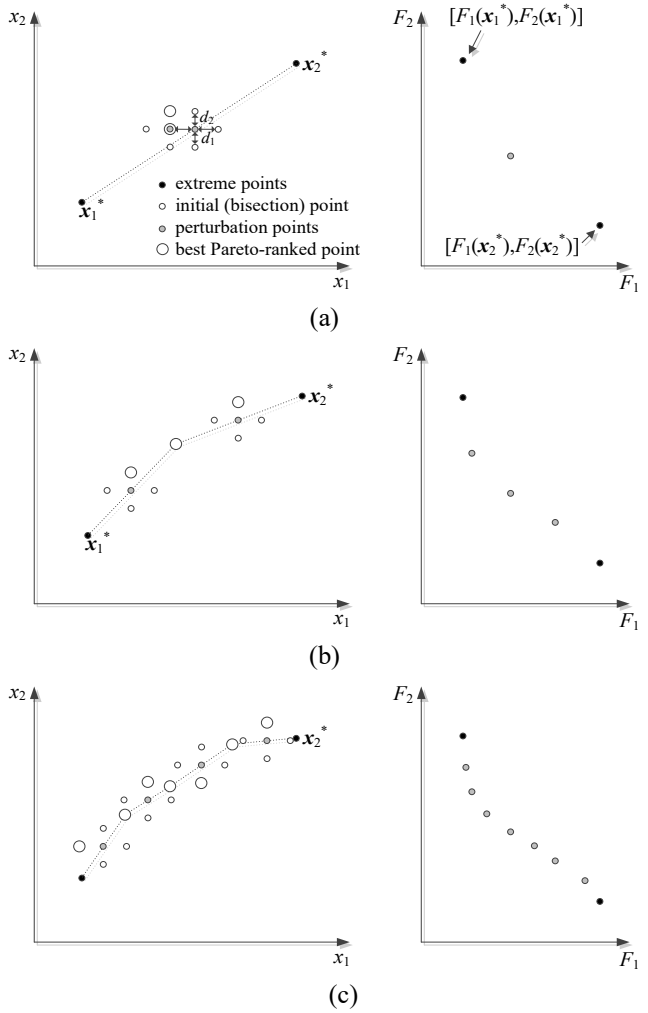

Figure 1: Pareto ranking bisection algorithm: conceptual illustration for generation of the low-fidelity Pareto set (left- and right-hand side plots represent, the search and the feature spaces, respectively): (a) first algorithm iteration – bisection of the line segment between the extreme Pareto designs and subsequent improvement of the candidate point through poll-search involving Pareto ranking (two iterations of the process are shown), (b) second algorithm iteration – bisection of the line segments between available Pareto designs and Pareto-ranking-based improvement of candidates (results obtianed after one iteration), (c) final agorithm iteration – bisection of segments between obtained designs and improvement of the candidates, as well as the final Pareto set.

The process (2) aims at improving the first objective without degrading the second one. The initial approximation of the optimal design for the refinement process is $\boldsymbol{x}_f^{(k)} = \boldsymbol{x}_c^{(k)}$. Typically, up to two iterations of the correction procedure are sufficient for convergence. It should be noted that the correction term $\boldsymbol{R}_s(\boldsymbol{x}) + [\boldsymbol{R}_f(\boldsymbol{x}_f^{(k)}) - \boldsymbol{R}_s(\boldsymbol{x}_f^{(k)})]$ ensures zero-order consistency, i.e., $\boldsymbol{R}_s(\boldsymbol{x}_f^{(k)}) = \boldsymbol{R}_f(\boldsymbol{x}_f^{(k)})$ at the beginning of each iteration. The utilized surrogate model is a second-order polynomial constructed from the low-fidelity model evaluations at $\boldsymbol{x}_c^{(k)}$ and star-distributed perturbations around it (with perturbation size set to $\boldsymbol{d}$). The computational cost of the refinement process corresponds to $2n + 1$ simulations of the low-fidelity model (for construction of the local approximation model) and only one evaluation of the high-fidelity per iteration (for OSM correction of the surrogate).

3 Design Example

This section provides numerical validation of the considered Pareto ranking bisection algorithm. The considered design example is a 17-variable uniplanar antenna operating in ultra-wideband frequency range. Discussion of the computational cost of the algorithm and its comparisons to the benchmark methods are also provided.

3.1 Structure Description

Consider the compact uniplanar antenna shown in Fig. 2 (Koziel and Bekasiewicz, 2016d). It consists of a fork-shaped driven element fed through a coplanar waveguide (CPW) and an open ground plane slot with tetragon-shaped planes allocated at both upper corners of the structure. The antenna is implemented on a 0.762 mm thick Taconic RF-35 dielectric substrate (ε_r = 3.5, tanδ = 0.0018). It is described by a 17-variable vector: $\boldsymbol{x} = [l_0\ l_1\ l_{3r}\ l_{4r}\ l_{5r}\ l_{f1}\ l_{f2}\ l_{f3r}\ l_{sr}\ w_1\ w_{f1}\ w_{f2}\ w_{f3}\ w_g\ w_{sr}\ w_{s1r}\ g]^T$. Parameters w_0 = 3.5 and s_0 = 0.16 remain fixed to ensure 50 ohm input impedance of the CPW feed. Relative dimensions are: $l_3 = (0.5w_0 + s + w_1)l_{3r}$, $l_4 = (l_1 - g - l_{f1} - l_{f2})l_{4r}$, $l_{f3} = (0.5l_{f2} - w_{f1})l_{f3r}$, $l_s = (w_1 - w_g)l_{sr}$, $w_s = (w_1 - w_g)w_{sr}$, $l_{22} = \max\{(l_1 - g - l_{f1} - l_{f2})l_{5r}, (0.5w_0 + s_0 + w_1)l_{5r}\}$, and $w_{s1} = l_0 w_{s1r}$. All dimensions are in mm.

The high-fidelity EM model $\boldsymbol{R}_f$ of the antenna (~3,200,000 hexahedral mesh cells, average simulation time: 20 min) and the low-fidelity EM model $\boldsymbol{R}_c$ (~650,000 mesh cells, simulation time: 230 s) are both implemented in CST Microwave Studio and simulated using its time domain solver (CST, 2013). For the sake of reliable simulation results, both models include the SMA connector.

The design objectives are: F_1 – minimization of the antenna reflection within 3.1 GHz to 10.6 GHz frequency band, and F_2 – reduction of antenna size defined as a $A \times B$ rectangle with $A = 2(s_0 + w_1) + w_0$ and $B = l_0 + l_1$ (cf. Fig. 2). The antenna topology is consistent within the following lower and upper bounds: $\boldsymbol{l}$ = [4 13 0.2 0.25 0.1 4 8 0.2 0 5 0.2 0.2 0.2 0.2 0.1 0 0.1]^T and $\boldsymbol{u}$ = [14 25 0.9 0.85 0.8 11 16 0.8 0.45 15 2.5 2 2.5 1.5 0.45 0.45 2]^T.

3.2 Results and Discussion

In the first step of the design process, the extreme Pareto designs $\boldsymbol{x}_1^*$ = [4.94 15.75 0.74 0.84 0.67 9.15 15.93 0.22 0 8.15 2.35 0.21 0.44 0.64 0.16 0.02 0.16]^T and $\boldsymbol{x}_2^*$ = [4 13.38 0.9 0.85 0.77 8.59 13.25 0.2 0.04 5.57 2.02 0.2 0.2 0.2 0.14 0.45 0.1]^T have been obtained using (1). Then, multi-objective optimization of the antenna has been performed using PRBA (setup: M = 3, $\boldsymbol{m}$ = [3 2 1]). Finally, the initial Pareto set has been refined using algorithm of Section 2.3. Comparison of the low- and the high-fidelity trade-off designs is shown in Fig. 3. It should be noted that the high-fidelity Pareto set ranges along F_1 from –13.3 dB to –9.9 dB. Moreover, the extreme Pareto design obtianed w.r.t. F_1 is dominated. Detailed dimensions of the selected antenna designs are gathered in Table 1, whereas their corresponding reflection characteristics are shown in Fig. 4.

The computational cost of the design process corresponds to 207 $\boldsymbol{R}_f$ model simulations (69 hours of CPU-time). The cost includes: 473 $\boldsymbol{R}_c$ and 207 $\boldsymbol{R}_c$ model simulations for identification of the extreme Pareto designs and PRBA-based optimization, respectively, as well as 245 $\boldsymbol{R}_c$ and 30 $\boldsymbol{R}_f$ model evaluations for refinement of the initial Pareto set.

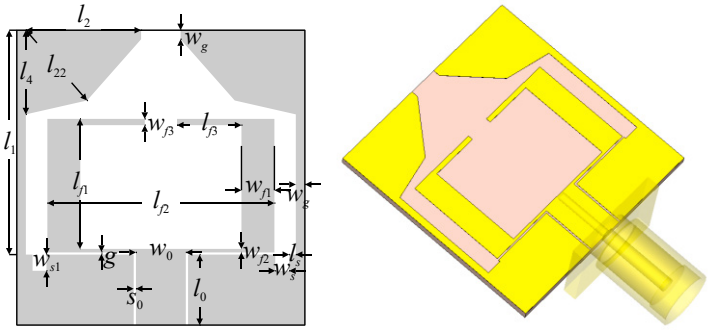

Figure 2: Geometry of the considered antenna. From left: top view and 3D view with SMA connector.

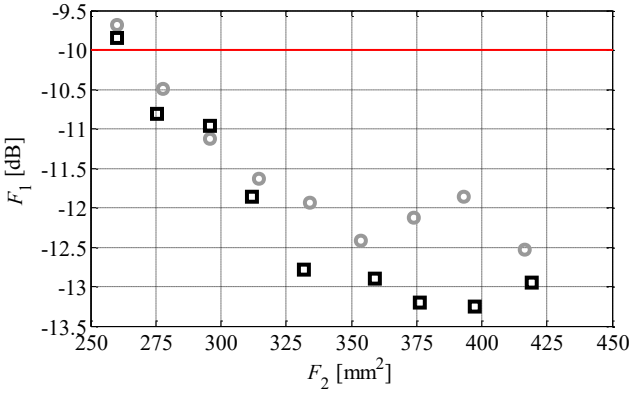

Figure 3: Comparison of the low-fidelity Pareto set obtained using PRBA (○) and high-fidelity set after the refinement (□).

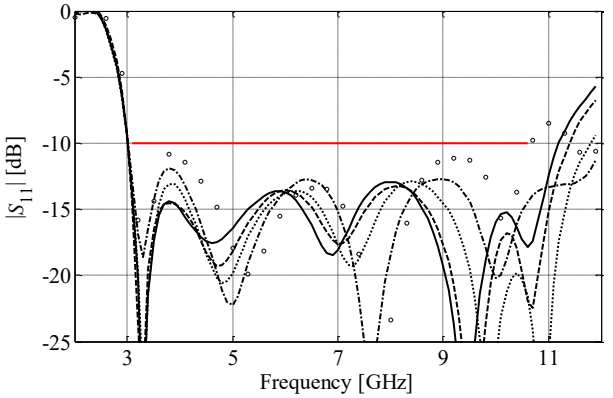

Figure 4: Frequency responses of the selected Pareto-optimal designs: $\boldsymbol{x}_f^{(1)}$ (—), $\boldsymbol{x}_f^{(2)}$ (– –), $\boldsymbol{x}_f^{(4)}$ (···), $\boldsymbol{x}_f^{(6)}$ (–·–), and $\boldsymbol{x}_f^{(8)}$ (◦◦◦).

Table 1: Dimensions of the High-Fidelity Antenna Designs

Objectives			Design variables																
No	F_1	F_2	l_0	l_1	l_{3r}	l_{4r}	l_{5r}	l_{f1}	l_{f2}	l_{f3r}	l_{sr}	w_1	w_{f1}	w_{f2}	w_{f3}	w_g	w_{sr}	w_{s1r}	g
1	–12.9	419	4.85	16.02	0.72	0.84	0.68	9.22	15.75	0.22	0.00	8.13	2.37	0.21	0.47	0.69	0.16	0.07	0.16
2	–13.3	397	4.82	15.59	0.74	0.84	0.69	9.05	15.42	0.22	0.01	7.83	2.34	0.21	0.44	0.61	0.16	0.12	0.15
4	–12.9	359	4.69	14.89	0.81	0.84	0.71	8.77	14.80	0.21	0.01	7.25	2.25	0.21	0.38	0.48	0.15	0.19	0.15
6	–11.9	312	4.34	14.24	0.87	0.85	0.76	8.71	14.22	0.21	0.03	6.48	2.11	0.20	0.29	0.36	0.15	0.35	0.12
8	–10.8	276	4.19	13.92	0.88	0.85	0.78	8.63	13.65	0.20	0.03	5.70	2.04	0.20	0.23	0.22	0.14	0.36	0.11

3.3 Comparisons with Benchmark Algorithms

PRBA has been compared to surrogate-assisted multi-objective evolutionary algorithm (SAMOEA; Koziel et al. 2014b), sequential domain patching (SDP) algorithm (Koziel and Bekasiewicz, 2016b), and Pareto front exploration (PFE) algorithm (Koziel and Bekasiewicz, 2016c) in terms of the computational cost and the quality of the obtained Pareto set. It should be noted that the comparisons have been performed only at the low fidelity model level. The correction process has been neglected as it affects the shape of the final representation of the Pareto front (see e.g., Fig. 3) and its cost is the same for all considered methods.

The SAMOEA-based optimization involves construction of the approximation model that is optimized by the metaheuristic algorithm. The model error constructed in search space defined by extreme designs obtained using method of Section 3.2 is 12% (2000 training samples) which makes it inappropriate for optimization. Therefore, model with acceptable an error of 3% (902 training samples) has been re-set in the region restricted using rotational space reduction method (Koziel and Bekasiewicz, 2016a).

The computational cost of multi-objective optimization by SAMOEA (setup: population size 500, number of iterations 50), SDP (setup: maximum number of intervals 16), PFE (setup: size threshold 20 mm^2) and PRBA is 1375, 1116, 825, and 680, respectively. The detailed cost breakdown is provided in Table 2. PRBA operation involves 17% less CPU-time compared to PFE. Moreover, the cost of the algorithm is almost 39% and over 50% lower compared to SDP and SAMOEA, respectively. Note that the cost of identifying the extreme designs for PFE is lower than for remaining methods, because it requires only one extreme point (here obtained with respect to minimum in-band reflection).

The comparison of low-fidelity Pareto sets obtained using considered algorithms is shown in Fig. 5. The discrepancy between the obtained designs along F_1 is below 1.5 dB, which is negligible from the practical point of view. Discontinuities of the set found using SAMOEA are a result of a narrow search space obtained using the rotational technique. As a consequence, part of the Pareto designs is allocated outside the approximation model and hence they cannot be identified. Notwithstanding, the results are in acceptable agreement. For the considered design structure, the PRBA not only features the lowest computational cost among compared algorithms but also if provides comparable approximation of the Pareto front.

4 Conclusions

In the paper, a Pareto ranking bisection algorithm has been utilized for rapid multi-objective optimization of a 17-parameter uniplanar UWB antenna structure. As demonstrated, a nine-element representation of the high-fidelity Pareto front has been obtained at a cost corresponding to only 207

simulations of the EM antenna model. The computational cost of the procedure (excluding the CPU-time required for the refinement of the initial Pareto set) is up to 50 percent lower compared to the state-of-the-art surrogate-assisted multi-objective optimization algorithms while providing similar accuracy. The obtained numerical results prove usefulness of the Pareto ranking bisection algorithm for optimization of many-parameter antennas. Our further work will focus on implementation of the method for optimization of other numerically demanding microwave and antenna structures with many adjustable parameters.

Acknowledgements

The authors would like to thank Computer Simulation Technology AG, Darmstadt, Germany, for making CST Microwave Studio available. This work was supported in part by the Icelandic Centre for Research (RANNIS) Grant 1502034051 and by National Science Centre of Poland Grant 2013/11/B/ST7/04325.

Table 2: Multi-Objective Optimization: Cost Breakdown

Algorithm	Identification of extreme Pareto designs	Multi-objective optimization	Total cost [$\boldsymbol{R}_c$]	Total cost [$\boldsymbol{R}_f$]	CPU-time [h]
SAMOEA	473	207	1375	263.5	87.8
SDP	473	690	1116	213.9	71.3
PFE	195	630	825	158.1	52.7
PRBA (this work)	473	902	680	130.3	43.4

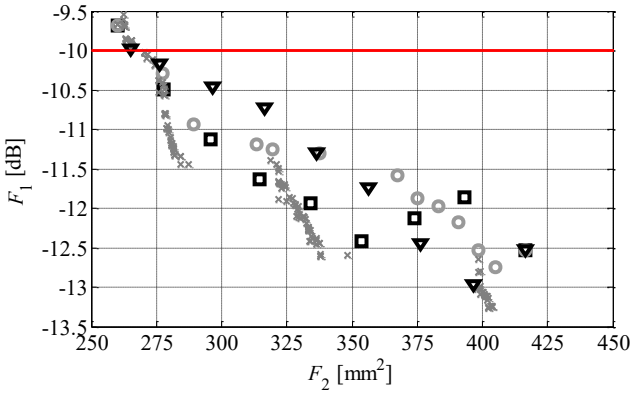

Figure 5: Comparison of the low-fidelity Pareto sets obtained using SAMOEA (×), SDP (○), PFE (∇), and PRBA (□).

References

Alsath, M.G.N., Kanagasabai, M. (2015). *Compact UWB monopole antenna for automotive communications*. IEEE Trans. Ant. Prop., 63, 4204-4208.

Bekasiewicz, A., Koziel, S. (2015). *Structure and Computationally-Efficient Simulation-Driven Design of Compact UWB Monopole Antenna*. IEEE Ant. Wireless Prop. Lett., 14, 1282-1285.

Conn, A., Scheinberg, K., Vincente, L.N. (2009). *Introduction to Derivative-Free Optimization*, MPS-SIAM Series on Optimization, Philadelphia,.

CST Microwave Studio, CST AG, Bad Nauheimer Str. 19, D-64289 Darmstadt, Germany, 2013.

Deb, K. (2001). *Multi-Objective Optimization Using Evolutionary Algorithms.* New York.

Ding, M., Jin, R., Geng, J., Wu, Q., Yang, G. (2008). *Auto-design of band-notched UWB antennas using mixed model of 2D GA and FDTD*. Electronics Lett., 44, 257-258.

Khan, M.S., Capobianco, A.-D., Iftikhar, A., Asif, S., Braaten, B.D. (2016). *A compact dual polarized ultrawideband multiple-input- multiple-output antenna*. Microw. Opt. Tech. Lett., 58, 163-166.

Li, G.L., Cheung, S.W., Yuk, T.I. (2013). *Compact MIMO antenna for portable devices in UWB applications*. IEEE Trans. Antennas Prop., 61, 4257-4264.

Li, T., Zhai, H., Li, G., Li, L., Liang, C. (2012). *Compact UWB bandnotched antenna design using interdigital capacitance loading loop resonator*. IEEE Antennas Wireless Prop. Lett., 11, 724–727.

Liu, L., Cheung, S.W., Weng Y.F., Yuk T.I. (2012). Cable effects on measuring small planar UWB monopole antennas. in M.A. Matin (ed.) *Ultra Wideband - Current Status and Future Trends*, Intech.

Koziel, S., Bandler, J.W. (2015). *Rapid yield estimation and optimization of microwave structures exploiting feature-based statistical analysis*. IEEE Trans. Microwave Theory Tech., 63, 107-114.

Koziel, S., Bekasiewicz, A. (2015). *Fast multi-objective optimization of narrowband antennas using RSA models and design space reduction.* IEEE Ant. Wireless Prop. Lett., 14, 450-453.

Koziel, S., Bekasiewicz, A. (2016a). *Fast multi-objective surrogate-assisted design of multi-parameter antenna structures through rotational design space reduction*. IET Microwaves, Ant. Prop., 10, 624-630.

Koziel, S., Bekasiewicz, A. (2016b). *Multi-objective antenna design by means of sequential domain patching*. IEEE Antennas Wireless Prop. Lett., 15, 1089-1092.

Koziel, S., Bekasiewicz, A. (2016c). *Rapid multi-objective antenna design using point-by-point Pareto set identification and local surrogate models*. IEEE Trans. Antennas Prop., vol. 64, 2551-2556.

Koziel, S., Bekasiewicz, A. (2016d). *A structure and simulation-driven design of compact CPW-fed UWB antenna.* IEEE Antennas Wireless Prop. Lett., 15, 750-753.

Koziel, S., Bekasiewicz, A. (2017). *Pareto ranking bisection algorithm for expedited multi-objective optimization of antenna structures.* IEEE Antennas Wireless Prop. Lett., 2017.

Koziel, S., Ogurtsov, S. (2013). *Multi-objective design of antennas using variable-fidelity simulations and surrogate models.* IEEE Trans. Ant. Prop., 61, 5931-5939.

Koziel, S. Ogurtsov, S. (2014). *Design optimization of antennas using electromagnetic simulations and adaptive response correction technique*. IET Microwaves, Ant. Prop., 8, 180-185.

Koziel, S., Ogurtsov, S., Szczepanski, S. (2012). *Rapid antenna design optimization using shape-preserving response prediction*. Bulletin of the Polish Academy of Sciences. Tech. Sci., 60, 143-149.

Koziel, S., Leifsson, L., Ogurtsov, S. (2013). *Reliable EM-driven microwave design optimization using manifold mapping and adjoint sensitivity*. Microwave Opt. Tech. Lett., 55, 809-813.

Koziel, S., Bekasiewicz, A., Couckuyt, I., Dhaene, T. (2014a). *Efficient multi-objective simulation-driven antenna design using co-kriging*. IEEE Trans. Antennas Prop., 62, 5900-5905.

Koziel, S., Bekasiewicz, A., Zieniutycz, W. (2014b). *Expedited EM-driven multi-objective antenna design in highly-dimensional parameter spaces*. IEEE Ant. Wireless Prop. Lett., 13, 631-634.

Kuwahara, Y. (2005). *Multiobjective optimization design of Yagi–Uda antenna*. IEEE Trans. Ant. Prop., 53, 1984–1992.

Martinez-Fernandez, J., Gil, J.M., Zapata, J. (2007). *Ultrawideband optimized profile monopole antenna by means of simulated annealing algorithm and the finite element method*. IEEE Trans. Ant. Prop., 55, 1826-1832.

Nocedal, J., Wright, S. (2006). *Numerical Optimization*, 2nd edition, Springer, New York.

Nouri, A., DadashZadeh, G.R. (2011). *A compact UWB band-notched printed monopole antenna with defected ground structure*. IEEE Antennas Wireless Prop. Lett., 10, 1178-1181.

Yang, X.S. (2013). *Multi-objective firefly algorithm for continuous optimization*. Engineering with Computers, 29, 175-184.